Oxidation of Ruthenium(II) Tris(2,2'-bipyridine) Ions by Thallic Ions in Nitric Acid, Mediated by Ruthenium Dioxide Hydrate: An Example of Reversible Heterogeneous Redox Catalysis

Andrew Mills* and Grant Meadows

Department of Chemistry, University College of Swansea, Singleton Park, Swansea SA2 8PP, Wales, U.K.

Received February 24, 1993

The kinetics of the oxidation of $Ru(bpy)_3^{2+}$ to $Ru(bpy)_3^{3+}$ by Tl^{3+} ions, catalyzed by a dispersion of $RuO_2 \cdot xH_2O$ in 3 mol dm^{-3} HNO_3, are reported as a function of $[Ru(bpy)_3^{2+}]$, $[Tl^{3+}]$, $[Tl^+]$, $[RuO_2 \cdot xH_2O]$, and temperature. The kinetics of $Ru(bpy)_3^{2+}$ oxidation fit an electrochemical model of redox catalysis involving electron transfer between the two electrochemically reversible redox couples, *i.e.* $Ru(bpy)_3^{3+}/Ru(bpy)_3^{2+}$ and Tl^{3+}/Tl^+, mediated by the dispersion of microelectrode particles of $RuO_2 \cdot xH_2O$. In this model, the rate of reaction is assumed to be controlled by the diffusion of $Ru(bpy)_3^{2+}$ toward, and $Ru(bpy)_3^{3+}$ away from, the catalyst particles. The Arrhenius activation energy for the catalyzed reaction is 25.9 ± 0.7 kJ mol^{-1}, and the changes in enthalpy and entropy for the reaction are 36 ± 2 kJ mol^{-1} and 127 ± 6 J mol^{-1} K^{-1}, respectively. This work describes a rare example of reversible heterogeneous redox catalysis.

Introduction

Heterogeneous catalysis of redox reactions is at the heart of many industrial processes, including the extraction of minerals from ores, electrodeless plating, chloralkali production, photographic development, and the descaling of industrial pipework.[1,2] It is also a vital ingredient in green plant photosynthesis, particularly photosystem II,[3] and many artificial solar to chemical energy conversion systems, especially those involving water-splitting.[4]

In many examples of heterogeneous redox catalysis,[1] the catalyst provides a surface which lowers the intrinsic barriers to the valence changes associated with one, or more, of the participating couples and provides a medium for electron transfer from one redox couple to another. Thus, the catalyst acts both as an anode for one couple and a cathode for the other with a direct short between the two "electrodes". This electrochemical approach to redox catalysis allows the prediction of the kinetics of the general single electron transfer redox reaction:

$$a\,Ox_2 + b\,Red_1 \rightarrow c\,Red_2 + d\,Ox_1 \qquad (1)$$

where *a*–*d* are the appropriate stoichiometric coefficients, provided the current–voltage curves for the two contributing couples are known and the couples act independently of one another;[1] the latter condition is known as the Wagner–Traud additivity principle.[1]

In the electrochemical approach to interpreting the observed kinetics of heterogeneous redox catalysis, a key concept is electrochemical reversibility and needs to be defined here. Thus, for a given electrode, the more electrochemically reversible a couple behaves, the faster the exchange of electrons between its oxidized and reduced forms occurs at the electrode.[4] A measure of this electron exchange rate is provided by the exchange current density, i_0, and typically,[5] for an electrochemically reversible reaction i_0 is $>10^{-6}$ A cm^{-2} and for an electrochemically irreversible reaction i_0 is $<10^{-10}$ A cm^{-2}.

Despite the importance of redox catalysis, detailed kinetic studies have only emerged during the last decade, prompted, most significantly, by the interest in the development of efficient artificial solar to chemical energy conversion systems and, therefore, the development of active essential redox catalysts.[4] The most dramatic examples of redox catalysis have usually involved the coupling of a highly irreversible redox reaction, such as the oxidation of water, to a highly reversible reduction reaction, such as the reduction of Ce(IV) or $Ru(bpy)_3^{3+}$ ions.[6,7]

In contrast to the above, examples of "reversible heterogeneous redox catalysis", which involves electron transfer between two electrochemically reversible redox couples mediated by a solid redox catalyst, are uncommon[8] largely because, in practice, the associated homogeneous (noncatalyzed) reaction is usually much faster than the heterogeneous (catalyzed) one.[5] Homogeneous redox reactions which fall in this category are often complementary and the intrinsic barriers to the valence changes involved are usually low. In contrast, the oxidation of $Ru(bpy)_3^{2+}$ by Tl^{3+}, *i.e.*

$$^1/_2Tl^{3+} + Ru(bpy)_3^{2+} \rightleftharpoons {}^1/_2Tl^+ + Ru(bpy)_3^{3+} \qquad (2)$$

is a noncomplementary redox reaction and the homogeneous self-exchange reaction between Tl^{3+} and Tl^+ is slow,[9,10] indicating a high intrinsic barrier to the overall valence change. However, the two different redox couples involved in reaction 2 are known to act reversibly at some macroelectrodes, such as platinized platinum electrodes.[11–14] Assuming that the electrochemical model is applicable, the latter feature opens up the possibility of being able to catalyze reaction 2 using a dispersion of particles which can act as microelectrodes for both the electrochemically reversible oxidation of $Ru(bpy)_3^{2+}$ to $Ru(bpy)_3^{3+}$ and the electrochemically reversible reduction of Tl^{3+} to Tl^+. In this work we report the results of a kinetic study of reaction 2 in 3 mol dm^{-3} HNO_3, mediated by a dispersion of the conductive metallic oxide redox catalyst, ruthenium dioxide hydrate, $RuO_2 \cdot xH_2O$.

(1) Spiro, M. *Chem. Soc. Rev.* **1986**, *15*, 141.
(2) Segal, M. G.; Sellers, R. M. *Advances in Inorganic and Bioinorganic Mechanisms*; Sykes, A. G., Ed.; Academic Press: London, 1984; pp 97–129.
(3) Barber, J.; Nakatani, H. Y.; Mansfield, R. *Isr. J. Chem.* **1981**, *21*, 243.
(4) Mills, A. *Chem. Soc. Rev.* **1989**, *18*, 285 and references therein.
(5) Spiro, M.; Ravnō, A. B. *J. Chem. Soc.* **1965**, 78.
(6) Mills, A.; Giddings, S.; Patel, I.; Lawrence, C. *J. Chem. Soc., Faraday Trans. 1* **1987**, *83*, 2331.
(7) Humphry-Baker, R.; Lilie, J.; Grätzel, M. *J. Am. Chem. Soc.* **1982**, *104*, 422.
(8) Freund, P. L.; Spiro, M. *J. Chem. Soc., Faraday Trans. 1* **1983**, *79*, 481.
(9) Roig, E.; Dodson, R. W. *J. Phys. Chem.* **1961**, *65*, 2175.
(10) Schwarz, H. A.; Comstock, D.; Yandell, J. K.; Dodson, R. W. *J. Phys. Chem.* **1974**, *78*, 488.
(11) Vetter, K. J.; Thiemke, G. *Z. Elektrochem.* **1960**, *64*, 805.
(12) Noyes, A. A.; Garner, C. S. *J. Chem. Soc.* **1936**, 1269.
(13) Miller, J. D.; Prince, R. H. *J. Chem. Soc. A* **1966**, 1048.
(14) Dwyer, F. P. *J. Proc. R. Soc. N.S.W.* **1949**, *83*, 134.

0020-1669/93/1332-3433$04.00/0

Experimental Section

Materials. The ruthenium(II) tris(2,2'-bipyridine) dichloride hexahydrate was purchased from Strem Chemicals UK, the nitrate salts of Tl(I) and Tl(III), *i.e.* $TlNO_3$ and $Tl(NO_3)_3 \cdot 3H_2O$, were obtained from Aldrich Chemicals UK, the $RuO_2 \cdot xH_2O$ (batch no. 061301B) was obtained from Johnson Matthey UK, and the concentrated nitric acid used to prepare the 3 mol dm^{-3} HNO_3 was purchased from BDH Chemicals UK. $RuO_2 \cdot xH_2O$ used in this work was a typical example of highly hydrated ruthenium(IV) oxide, *i.e.* high % H_2O content (% H_2O measured by TGA = 24%), high surface area (specific surface area measured by the BET technique = 80 $m^2\ g^{-1}$), amorphous to X-rays, and forming large aggregated particles in aqueous solution (average diameter measured by dynamic light scattering = 6.1 ● 1.4 μm). Further characterization details concerning $RuO_2 \cdot xH_2O$ are given elsewhere.[6] The choice of 3 mol dm^{-3} HNO_3 as the reaction medium was made to ensure that the majority of Tl(I) and Tl(III) ions present in the solution were in the form of Tl^+ and Tl^{3+}, respectively, and, therefore, that the kinetics of reaction 2 were not complicated by the presence of a substantial proportion of hydrolysis derivatives,[9] such as $Tl(OH)^{2+}$. In all cases the chemicals were of the highest purity available and were used as received. The water used to prepare solutions was doubly distilled and deionized.

Methods. The kinetics of the oxidation of $Ru(bpy)_3^{2+}$ by Tl^{3+} ions, mediated by ruthenium dioxide hydrate, $RuO_2 \cdot xH_2O$, in 3 mol dm^{-3} HNO_3, *i.e.* reaction 2, were studied spectrophotometrically by monitoring the change in absorbance at 452 nm, due to changes in the concentrations of $Ru(bpy)_3^{2+}$ (molar absorptivity = 12 900 $dm^3\ mol^{-1}\ cm^{-1}$) and $Ru(bpy)_3^{3+}$ (molar absorptivity = 601 $dm^3\ mol^{-1}\ cm^{-1}$), as a function of time. For each kinetic run, the associated normalized absorbance change, A^*, *versus* time profile was calculated from the recorded absorbance (452 nm) *versus* time profile using the working equation:

$$A^* = (A_t - A_{eq})/(A_0 - A_{eq}) \quad (3)$$

where A_t, A_{eq}, and A_0 are the absorbances at 452 nm at the following times: (i) time t, (ii) the end of the reaction (the equilibrium absorbance), and (iii) the start of the reaction (the initial absorbance), respectively. In all our work, at any time t during the reaction, the combined concentrations of $Ru(bpy)_3^{2+}$ and $Ru(bpy)_3^{3+}$ were assumed to be equal to the initial concentration of $Ru(bpy)_3^{2+}$, *i.e.* $[Ru(bpy)_3^{2+}]_0 = ([Ru(bpy)_3^{2+}]_t + [Ru(bpy)_3^{3+}]_t)$. As a result, from Beer's law and eq 3, the following expression relating A^* to $[Ru(bpy)_3^{2+}]_t$ was assumed to hold:

$$A^* = \{[Ru(bpy)_3^{2+}]_t - [Ru(bpy)_3^{2+}]_{eq}\}/\{[Ru(bpy)_3^{2+}]_0 - [Ru(bpy)_3^{2+}]_{eq}\} \quad (4)$$

Absorbance measurements were made using a Perkin-Elmer Lambda 3 double-beam spectrophotometer.

For each set of kinetic runs the stock dispersion of $RuO_2 \cdot xH_2O$ was made up fresh on the day. The initial dispersion of the catalyst was achieved by subjecting the stock to 5 min of ultrasound from an ultrasound bath; thereafter the stock dispersion exhibited a constant catalytic activity over a 12-h period at least.

Theory

From the results of separate electrochemical studies carried out by others[11-14] on the Tl^{3+}/Tl^+ and $Ru(bpy)_3^{3+}/Ru(bpy)_3^{2+}$ couples using platinum macroelectrodes, it appears that both couples are electrochemically reversible, *i.e.* exhibit exchange current densities > 10^{-6} A cm^{-2}, and it is likely that a similar situation will apply to the microelectrode, powder particles of $RuO_2 \cdot xH_2O$, used in this work. Thus, assuming electrochemical reversibility for the Tl^{3+}/Tl^+ and $Ru(bpy)_3^{3+}/Ru(bpy)_3^{2+}$ couples, both (i) the two successive single electron transfer steps, *i.e.*

$$Tl^{3+} + e^- + M \rightleftharpoons M\text{–}Tl^{2+} \quad (5)$$

$$M\text{–}Tl^{2+} + e^- \rightleftharpoons M + Tl^+ \quad (6)$$

and (ii) the single electron transfer step, *i.e.*

$$Ru(bpy)_3^{2+} - e^- \overset{Pt}{\rightleftharpoons} Ru(bpy)_3^{2+} \quad (7)$$

respectively, will occur rapidly enough to maintain a Nernstian equilibrium at the surface of the electrode. In reaction 5, M is an electrode reaction site which is able to stabilize the usually highly reactive species Tl^{2+}; the surface coverage of M–Tl^{2+} is assumed to be low.[11]

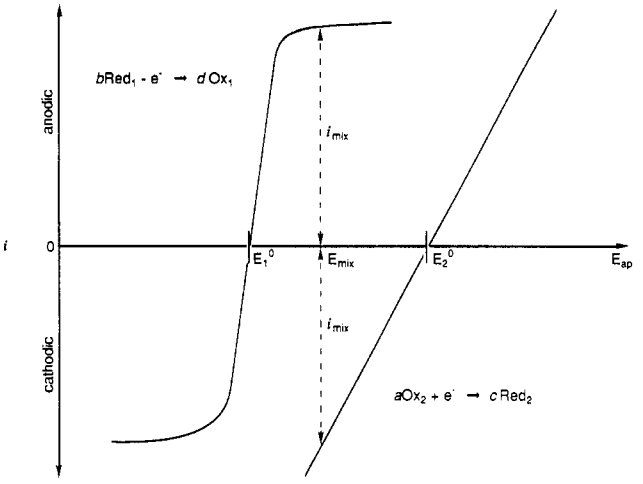

Figure 1. Schematic illustration of the current–voltage curves for two highly reversible redox couples, *i.e.* Ox_1/Red_1 (at a low concentration) and Ox_2/Red_2 (at a high concentration), respectively, present in the same solution and coupled together *via* redox catalysis. In the electrochemical model of redox catalysis the microelectrode particles are poised at a mixture potential, E_{mix}, so that the anodic current flowing through the catalyst particles, due to the oxidation of Red_1, is equal to the cathodic current, due to the reduction of Ox_2; both currents are numerically equal to the mixture current, i_{mix}.

The rather complex electrochemical equations associated with catalysis of the general redox reaction 1, involving two reversible redox couples, have been described very well by Freund and Spiro.[8] In our work some simplification of these equations can be made, including the approximate invariance of $[Ox_2]$ and $[Red_2]$ during most kinetic runs, since the concentrations of Ox_2 (Tl^{3+}) and Red_2 (Tl^+) are usually much greater than those of Red_1 ($Ru(bpy)_3^{2+}$) and Ox_1 ($Ru(bpy)_3^{3+}$), *i.e.* typically >50 times. Thus, under these conditions, it is likely that the mixture potential on the catalyst particles, *i.e.* E_{mix}, is fixed and given by the Nernst equation for the Ox_2/Red_2 couple, *i.e.*

$$E_{mix} = E^\circ{}_2 + (RT/F)\ \ln\{[Ox_2]_0^a/[Red_2]_0^c\} \quad (8)$$

Given the assumption that the Ox_1/Red_1 couple is electrochemically reversible and that the diffusion of Red_1 to the electrode and Ox_1 away from the electrode determine the overall rate of reaction, it follows that the mixture potential, E_{mix}, and mixture current, i_{mix}, are related by the expression:

$$E_{mix} = E^\circ{}_1 + \frac{RT}{F}\ln\left(\frac{[Ox_1]^d}{[Red_1]^b}\right) + \frac{RT}{F} \times \ln\left\{\left(1 + \frac{i_{mix}}{L_{OX1}}\right)^d \Big/ \left(1 + \frac{i_{mix}}{L_{RED1}}\right)^b\right\} \quad (9)$$

where L_{OX1} and L_{RED1} are the diffusion-controlled currents associated with the reduction of Ox_1 and oxidation of Red_1, respectively; a schematic illustration of the typical current–voltage curves for the two redox couples, and the resulting mixture current and potential, at some arbitrary time during the reaction, is illustrated in Figure 1.

If we assume the mass-transfer coefficients for the latter two species have the same value, k_d, then L_{OX1} and L_{RED1} can be defined by the following expressions:

$$L_{OX1} = Fk_dA_{cat}[Ox_1] = K[Ox_1] \quad (10)$$

$$L_{RED1} = Fk_dA_{cat}[Red_1] = K[Red_1] \quad (11)$$

where $K = Fk_dA_{cat}$ and A_{cat} is the effective catalyst surface area per unit volume of solution.

In the redox system under study, *i.e.* reaction 2, $a = c = {}^1/_2$, $d = b = 1$, $Ox_1 = Ru(bpy)_3^{3+}$, $Red_1 = Ru(bpy)_3^{2+}$, $Ox_2 = Tl^{3+}$, and $Red_2 = Tl^+$. At any time t during the reaction, the concentration of $Ru(bpy)_3^{3+}$ will be given by the expression

$$[Ru(bpy)_3^{3+}]_t = [Ru(bpy)_3^{2+}]_0 - [Ru(bpy)_3^{2+}]_t \quad (12)$$

With combination of eqs 8–12, the following simple expression can be derived for the mixture current at any time t during the redox reaction:

$$i_{mix,t} = K[Ru(bpy)_3^{2+}]_t - K[Ru(bpy)_3^{2+}]_0/(1 + \phi) \quad (13)$$

where the parameter ϕ is defined by the expression

$$\phi = ([Tl^{3+}]_0/[Tl^+]_0)^{1/2} \exp\{(E^\circ\{Tl^{3+}/Tl^+\} - E^\circ\{Ru(bpy)_3^{3+}/Ru(bpy)_3^{2+}\})F/RT\} \quad (14)$$

When the system reaches equilibrium, then $i_{mix,t} = 0$, and from eq 13 it follows

$$[Ru(bpy)_3^{3+}]_{eq}/[Ru(bpy)_3^{2+}]_{eq} = ([Tl^{3+}]_0/[Tl^+]_0)^{1/2} \exp\{(E^\circ\{Tl^{3+}/Tl^+\} - E^\circ\{Ru(bpy)_3^{3+}/Ru(bpy)_3^{2+}\})F/RT\} \quad (15)$$

Combination of eqs 13–15 leads to the expression

$$i_{mix,t} = K([Ru(bpy)_3^{2+}]_t - [Ru(bpy)_3^{3+}]_{eq}) = -F(d[Ru(bpy)_3^{2+}]/dt) \quad (16)$$

In reaction 2, from eqs 3 and 4, at any time t during the reaction the experimentally determined parameter A^* is related directly to $([Ru(bpy)_3^{2+}]_t - [Ru(bpy)_3^{2+}]_{eq})$ and, therefore, to the rate of reaction, $d[Ru(bpy)_3^{2+}]/dt$. It follows from eq 16 that a prediction of the model is that the rate of reaction will be first-order with respect to A^*, *i.e.* a plot of ln A^* *versus* t will be a good straight line of gradient $-k_1$, and the associated first-order rate constant, k_1, will be related to the model parameters k_d and A_{cat} *via* the expression

$$k_1 = k_d A_{cat} \quad (17)$$

From eq 17 it follows that the measured first-order rate constant, k_1, will be proportional to $[RuO_2{\cdot}xH_2O]$ and independent of $[Tl^+]$ and $[Tl^{3+}]$.

In contrast to the kinetics predicted by the electrochemical model, it has been found[13] that the kinetics of the homogeneous (noncatalyzed) version of reaction 1 are irreversible, first-order with respect to $[Ru(bpy)_3^{2+}]$ and $[Tl^{3+}]$, and independent of $[Tl^+]$ and yield an activation energy, 96 kJ mol^{-1}, which is *ca.* 5–6 times greater than that for a diffusion-controlled reaction (15–19 kJ mol^{-1}).[15,16] The kinetics for the homogeneous version of reaction 2 have been interpreted[9] in terms of the following mechanism:

$$Ru(bpy)_3^{2+} + Tl^{3+} \rightleftharpoons Ru(bpy)_3^{3+} + Tl^{2+} \quad (18)$$

$$Ru(bpy)_3^{2+} + Tl^{2+} \xrightarrow[fast]{} Ru(bpy)_3^{3+} + Tl^+ \quad (19)$$

The formation of Tl^{2+} is a common feature of many noncomplementary reactions involving the Tl^{3+}/Tl^+ couple, and in some cases it has been possible to determine fundamental rate constants involving this species by pulse radiolysis.[17,18]

Results and Discussion

In all the kinetic runs, the associated A^* *versus* t profile, typically defined by 1000 data points, gave an excellent fit to first-order kinetics over $2^1/_2$ half-lives, *i.e.* with a correlation coefficient (r) >0.9990. The observation of first-order kinetics for reaction 2, with respect to $[Ru(bpy)_3^{2+}]$, is consistent with the electrochemical model developed above; see eq 16. The measured first-order rate constant for the catalyzed reaction was found to be typically *ca.* 30 times greater than that for the homogeneous version of reaction 2, determined under the same reaction conditions.

Table I. Variation in k_1 and $[Ru(bpy)_3^{3+}]_{eq}/[Ru(bpy)_3^{2+}]_{eq}$ as a Function of $[Tl^{3+}]_0$ and $[Tl^+]_0$

$[Tl^{3+}]_0$/ 10^{-3} mol dm^{-3}	$[Tl^+]_0$/ 10^{-3} mol dm^{-3}	k_1/ 10^{-2} s^{-1}	$\{[Ru(bpy)_3^{3+}]_{eq}/[Ru(bpy)_3^{2+}]_{eq}\}$
No Catalyst: Fixed $[Tl^{3+}]_0$, Fixed $[Tl^+]_0$			
3.6	3.6	0.05	
Fixed $[Tl^{3+}]_0$, Variable $[Tl^+]_0$			
3.6	3.6	1.10	2.34
3.6	2.9	1.11	2.65
3.6	2.2	1.00	3.15
3.6	1.5	1.11	3.91
3.6	0.7	1.06	5.75
3.6	0.4	1.11	8.40
3.6	0.0	1.08	
Variable $[Tl^{3+}]_0$, Fixed $[Tl^+]_0$			
3.6	3.6	1.12	2.37
2.9	3.6	1.13	2.10
2.2	3.6	0.97	1.76
1.5	3.6	0.92	1.35
0.7	3.6	0.75	1.24
0.4	3.6	0.64	0.33

In one set of experiments, the effect upon the kinetics of reaction 2 of different initial concentrations of Tl^{3+} ions, $[Tl^{3+}]_0$, varied over the range $(3.6–0.4) \times 10^{-3}$ mol dm^{-3}, with a fixed initial high concentration of Tl^+ ions, $[Tl^+]_0$, $= 3.6 \times 10^{-3}$ mol dm^{-3}, was studied. In this work the reaction conditions were otherwise as for a typical experiment, *i.e.* $[Ru(bpy)_3^{2+}]_0 = 7.1 \times 10^{-5}$ mol dm^{-3}, $[RuO_2{\cdot}xH_2O] = 18$ μg cm^{-3}, $[HNO_3] = 3$ mol dm^{-3}, and $T = 30$ °C, and from the A^* *versus* t profiles values for k_1 were determined as a function of $[Tl^{3+}]_0$. In addition, in the set of experiments described above, at the end of each kinetic run, the equilibrium absorbance at 452 nm was measured, and this information, combined with the knowledge of the molar absorptivities of $Ru(bpy)_3^{3+}$ and $Ru(bpy)_3^{2+}$ at 452 nm, allowed the calculation of the ratio, $[Ru(bpy)_3^{3+}]_{eq}/[Ru(bpy)_3^{2+}]_{eq}$, for that kinetic run. The results of all this work, *i.e.* the experimentally determined variation in k_1, and $[Ru(bpy)_3^{3+}]_{eq}/[Ru(bpy)_3^{2+}]_{eq}$, as a function of $[Tl^{3+}]_0$, are reported in Table I.

From the results in Table I, it appears that there may be some dependence of the rate of reaction 2 upon $[Tl^{3+}]_0$. However, a plot of $\ln(k_1)$ *versus* $\ln([Tl^{3+}]_0)$ reveals a straight line ($r = 0.9924$) with a gradient of only $(2.6 \pm 0.2) \times 10^{-1}$, indicating that in this set of experiments the observed dependence of k_1 upon $[Tl^{3+}]$ is slight, if at all. A lack of dependence of k_1 upon $[Tl^{3+}]$ is in clear distinction from that found by others for the homogeneous reaction, *i.e.* where k_1 is proportional to $[Tl^{3+}]_0$, but is in full agreement with the electrochemical model; see eq 16.

In a separate set of experiments, the effect upon the kinetics of reaction 2 of different initial concentrations of Tl^+ ions $\{[Tl^+]_0 = (3.6–0.4) \times 10^{-3}$ mol dm$^{-3}\}$, with a fixed initial high concentration of Tl^{3+} ions ($[Tl^{3+}]_0 = 3.6 \times 10^{-3}$ mol dm^{-3}), was studied. The experimentally determined variations in k_1 and $[Ru(bpy)_3^{3+}]_{eq}/[Ru(bpy)_3^{2+}]_{eq}$, as a function of $[Tl^+]_0$, are reported in Table I. From the results in Table I, it appears that k_1 is largely independent of $[Tl^+]_0$, and this is consistent with the electrochemical model, which predicts that the rate of reaction 2 will be independent of $[Tl^+]_0$; see eq 14.

The electrochemical model predicts, *via* eq 15, that a plot of $\ln\{[Ru(bpy)_3^{3+}]_{eq}/[Ru(bpy)_3^{2+}]_{eq}\}$ *versus* $\ln([Tl^{3+}]_0/[Tl^+]_0)$ of the data in Table I will be a good straight line with a gradient $= {}^1/_2$ and intercept $= (E^\circ\{Tl^{3+}/Tl^+\} - E^\circ\{Ru(bpy)_3^{3+}/Ru$-

(15) Wilkinson, F. *Chemical Kinetics and Reaction Mechanisms*; Van Nostrand Reinhold: London, 1981; p 140.
(16) Moore, J. W.; Pearson, R. G. *Kinetics and Mechanism*; J. Wiley: New York, 1981; p 239.
(17) Schwarz, H. A.; Dodson, R. W. *J. Phys. Chem.* **1976**, *80*, 2543.
(18) Schwarz, H. A.; Dodson, R. W. *J. Phys. Chem.* **1984**, *88*, 3643.

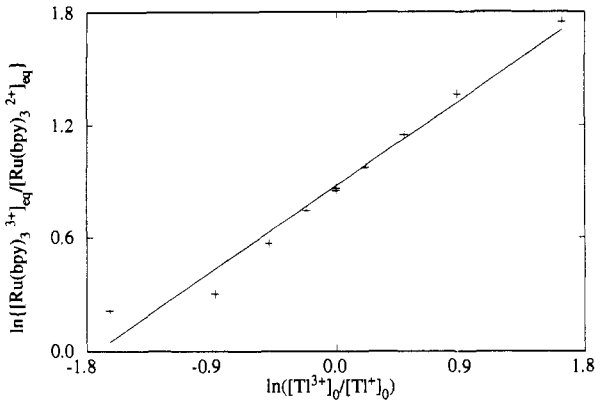

Figure 2. Plot of $\ln\{[Ru(bpy)_3^{3+}]_{eq}/[Ru(bpy)_3^{2+}]_{eq}\}$ *versus* $\ln([Tl^{3+}]_0/[Tl^+]_0)$ using the results given in Table I. Typical reaction conditions were as follows: 2.59 cm^3 of reaction solution, comprising, initially (t = 0), $[Ru(bpy)_3^{2+}]_0 = 7.1 \times 10^{-5}$ mol dm^{-3}; $[RuO_2{\cdot}xH_2O] = 18$ μg cm^{-3}; $[Tl^+]_0 = [Tl^{3+}]_0 = 3.6 \times 10^{-3}$ mol dm^{-3}, in a 1-cm cell with T = 30 °C. A least-squares analysis of the line of best fit to the data (solid line) revealed the following: $n = 10$, $m = 0.506 \pm 0.030$, $c = 0.88 \pm 0.03$, and $r = 0.9861$.

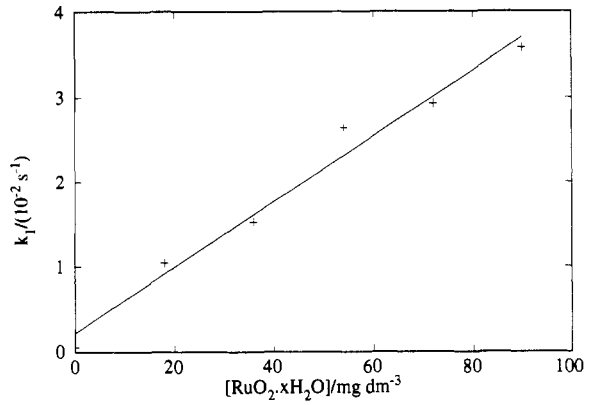

Figure 3. Plot of k_1 *versus* $[RuO_2{\cdot}xH_2O]$ with all other reaction conditions as for the typical reaction in Figure 2. A least-squares analysis of the line of best fit to the data (solid line) revealed the following: $n = 6$, $m = (3.88 \pm 0.28) \times 10^{-4}$ dm^3 mg^{-1} s^{-1}, $c = (2.18 \pm 1.54) \times 10^{-3}$ s^{-1}, and $r = 0.9895$.

$(bpy)_3^{2+}\})F/RT$; this plot is illustrated in Figure 2, and the good fit of the data to a straight line, gradient = 0.51, supports the prediction of the electrochemical model. From the intercept of the straight line of best fit to the data in Figure 2, a value for $(E^\circ\{Tl^{3+}/Tl^+\} - E^\circ\{Ru(bpy)_3^{3+}/Ru(bpy)_3^{2+}\}) = 23 \pm 1$ mV for T = 30 °C was calculated, and since the value of $E^\circ(Tl^{3+}/Tl^+)$ is known to be 1.230 V *versus* NHE,[12] it follows that $E^\circ\{Ru(bpy)_3^{3+}/Ru(bpy)_3^{2+}\} = 1.207$ V *versus* NHE. This calculated value for $E^\circ\{Ru(bpy)_3^{3+}/Ru(bpy)_3^{2+}\}$ is not that much smaller than that reported previously by others[11] for this couple (1.222 V) in 3 mol dm^{-3} HNO_3.

In another set of experiments, k_1 for reaction 2 was determined as a function of catalyst concentration, $[RuO_2{\cdot}xH_2O]$, over the range 18–90 μg cm^{-3}, with the other reaction conditions as for a typical experiment; *vide supra*. The plot of the results in the form k_1 *versus* $[RuO_2{\cdot}xH_2O]$ yields a good straight line with a near zero intercept, see Figure 3, and this finding is in agreement with the electrochemical model which predicts that k_1 will be directly proportional to A_{cat}, which, in turn, will be proportional to $[RuO_2{\cdot}xH_2O]$.

In a final set of experiments, the variations in k_1 and $[Ru(bpy)_3^{3+}]_{eq}/[Ru(bpy)_3^{2+}]_{eq}$ were measured as a function of reaction temperature over the range 14–39 °C, with all other reaction conditions as for a typical experiment. Figure 4a illustrates a selection of the different A_t/A_0 (see eq 3) *versus* time plots determined in this set of experiments. Using this data an

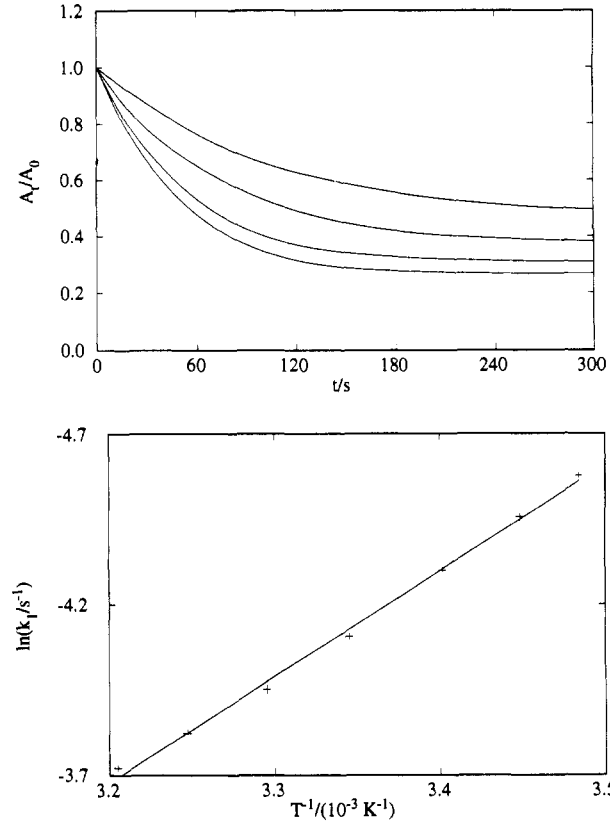

Figure 4. (a) Top: Selection of the A_t/A_0 *versus* time profiles recorded for reaction 2 at different temperatures but otherwise under the same typical reaction conditions as in Figure 2. The different profiles correspond (from top to bottom) to the following different temperatures: 14, 21, 30.5, and 35 °C. (b) Botton: Arrhenius plot of the different values of k_1 determined as a function of reaction temperature. A least-squares analysis of the line of best fit to the data (solid line) revealed the following: $n = 7$, $m = -(3.11 \pm 0.08) \times 10^3$ K, $c = 6.28 \pm 0.27$, and r = 0.9983.

Arrhenius plot of $\ln(k_1)$ *versus* T^{-1} was constructed which yielded a good straight line, as illustrated in Figure 4b. From the gradient of the line of best fit to the data in the Arrhenius plot, an activation energy for reaction 2 of 25.9 ± 0.7 kJ mol^{-1} was calculated, which is higher than that predicted by the electrochemical model, *i.e.* an activation energy for a diffusion-controlled reaction, *i.e.* 15–19 kJ mol^{-1} in water.[15,16] This discrepancy may be due, in part at least, to a marked increase in the initially very low fraction of k_1 due to the homogeneous reaction with increase in temperature; as noted previously, the homogeneous reaction has a high activation energy.[13]

From the data illustrated in Figure 4a, it is clear that the equilibrium ratio, $[Ru(bpy)_3^{3+}]_{eq}/[Ru(bpy)_3^{2+}]_{eq}$, is a function of temperature, as indicated by eq 15 of the electrochemical model. A plot of the measured equilibrium data, in the form $\ln\{[Ru(bpy)_3^{3+}]_{eq}/[Ru(bpy)_3^{2+}]_{eq}\}$ *versus* T^{-1}, gave a good straight line, as illustrated in Figure 5 and as predicted by the electrochemical model, *via* the combination of eq 15 with the following basic thermodynamic expressions for reaction 2: change in Gibbs free energy = (change in enthalpy) – T(change in entropy) = $-F\{E^\circ(Tl^{3+}/Tl^+) - E^\circ(Ru(bpy)_3^{3+}/Ru(bpy)_3^{2+})\}$. Values for the changes in enthalpy and entropy for reaction 2 of 36 ± 2 kJ mol^{-1} and 127 ± 6 J mol^{-1} K^{-1}, respectively, were calculated from the gradient {=–(change in enthalpy)/R} and intercept {=(change in entropy)/R} of the line of best fit illustrated in Figure 5. Using this thermodynamic data for reaction 2, it is possible to calculate a value for $(E^\circ\{Tl^{3+}/Tl^+\} - E^\circ\{Ru(bpy)_3^{3+}/Ru(bpy)_3^{2+}\})$, at 30 °C, of 27 ± 1 mV, which compares favorably with the earlier estimate of 23 ± 1 mV.

Additional experiments confirmed the feature of reversibility associated with the catalyzed version of reaction 2. Thus the

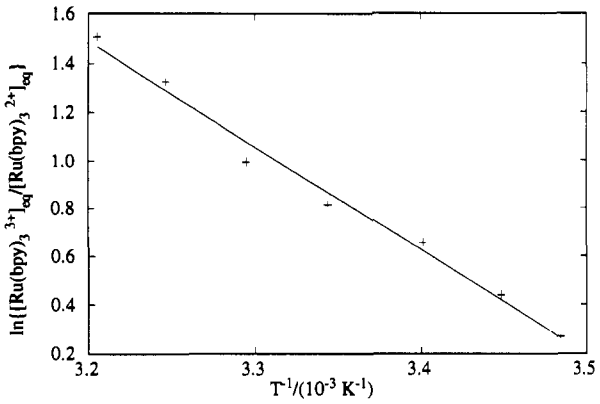

Figure 5. Plot of $\ln\{[Ru(bpy)_3^{3+}]_{eq}/[Ru(bpy)_3^{2+}]_{eq}\}$ *versus* T^{-1}, using the equilibrium data generated from the experiments carried out in Figure 4. A least-squares analysis of the line of best fit to the data (solid line) revealed the following: $n = 7$, $m = -(4.31 \pm 0.21) \times 10^3$ K, $c = 15.3 \pm 0.7$, and $r = 0.9943$.

addition of further amounts of Tl^+ to the final equilibrium mixture readily shifts the equilibrium back toward a reactant-rich mixture at a rate, and to an extent, which was fully predicted by the electrochemical model. Further research has shown that samples of highly hydrated ruthenium(IV) oxide obtained from chemical companies other than Johnson Matthey, such as Aldrich, Alfa, and Strem, or prepared by the aerobic alkaline hydrolysis of $RuCl_3 \cdot nH_2O$, are also able to catalyze reaction 2 and that the kinetics of catalysis exhibit the same features as described above.

Samples of $RuO_2 \cdot xH_2O$ exposed to a solution of Tl^{3+} ions, filtered, washed, and then introduced into a solution of $Ru(bpy)_3^{2+}$ were not able to oxidize $Ru(bpy)_3^{2+}$ to $Ru(bpy)_3^{3+}$. This latter result, along with more recent findings, *vide infra*, argues against an alternative mechanism of catalysis in which the surface of the $RuO_2 \cdot xH_2O$ is initially oxidized by Tl^{3+} ions and the oxidized surface of the catalyst is then responsible for the oxidation of the $Ru(bpy)_3^{2+}$ ions.

We have recently established that finely divided platinum black powder is also able to catalyze reaction 2 in exactly the same manner as found for $RuO_2 \cdot xH_2O$ and with a measured activation energy, (16.6 ± 1.4) kJ mol^{-1}, which is consistent with the reaction being diffusion-controlled. This latter finding provides support for the electrochemical model which predicts that any material, on which the Tl^{3+}/Tl^+ and $Ru(bpy)_3^{3+}/Ru(bpy)_3^{2+}$ couples appear electrochemically reversible, should exhibit the same features of catalysis as $RuO_2 \cdot xH_2O$.

Conclusion

The oxidation of $Ru(bpy)_3^{2+}$ to $Ru(bpy)_3^{3+}$ by Tl^{3+} ions in 3 mol dm^{-3} HNO_3 is catalyzed by a dispersion of $RuO_2 \cdot xH_2O$. The kinetics of catalysis fit an electrochemical model of redox catalysis in which electron transfer is between two highly reversible redox couples and is mediated by a dispersion of microelectrode particles of $RuO_2 \cdot xH_2O$. The rate of reaction is controlled by the diffusion of $Ru(bpy)_3^{2+}$ toward, and $Ru(bpy)_3^{3+}$ away from, the microelectrode particles. The Arrhenius activation energy for the catalyzed reaction is 25.9 ± 0.7 kJ mol^{-1}, and the changes of enthalpy and entropy are 36 ± 2 kJ mol^{-1} and 127 ± 6 J mol^{-1} K^{-1}, respectively. This work describes a rare, classic sample of reversible redox catalysis.

Acknowledgment. We thank the SERC for supporting one of us (G.M.) *via* a Quota award.